Received: 11 November 2020 | Revised: 2 February 2021 | Accepted: 1 March 2021

DOI: 10.1049/bsb2.12006

Biosurface and Biotribology

The Institution of Engineering and Technology WILEY

ORIGINAL RESEARCH PAPER

Effects of UHMWPE viscoelasticity on the squeeze-film lubrication of hip replacements

Xianjiu Lu[1] | Qingen Meng[2] | Zhongmin Jin[1,2,3]

[1]State Key Laboratory for Manufacturing Systems Engineering, Xi'an Jiaotong University, Xi'an, Shaanxi, China

[2]School of Mechanical Engineering, University of Leeds, Leeds, UK

[3]School of Mechanical Engineering, Tribology Research Institute, Southwest Jiaotong University, Chengdu, Sichuan, China

Correspondence

Zhongmin Jin, State Key Laboratory for Manufacturing Systems Engineering, Xi'an Jiaotong University, 710054, Xi'an, Shaanxi, China.
Email: zmjin@mail.xjtu.edu.cn

Funding information

National Science and Technology Supporting Programme, Grant/Award Number: 2012BAI18B00; National Science Foundation of China, Grant/Award Number: 51323007

Abstract

Many studies have been performed to analyse the lubrication of artificial joints since the pioneer work by the late Professor Duncan Dowson. However, the viscoelastic deformation of one of the most widely used bearing materials, ultra-high-molecular-weight polyethylene (UHMWPE), has only been considered recently. The described study attempted to investigate the effect of UHMWPE viscoelasticity on the elastohydrodynamic lubrication of such a soft artificial hip replacement under squeeze-film motion. A transient viscoelastic squeeze-film lubrication model of a typical hip implant was developed and solved to obtain the film thickness and pressure distributions. A boundary film thickness was adopted to consider the direct and indirect lubricant contact conditions. The results showed that the viscoelasticity had marked effects on the squeeze-film lubrication performance of UHMWPE artificial hip joints. The minimum film thickness in the viscoelastic model was smaller than that of the elastic model, causing an earlier direct contact. However, the film thickness within the central contact region in the viscoelastic model was greater than that of the elastic model due to the restricted flow of the lubricant, therefore enhancing the lubricating effect and particularly with a short relaxation time and mechanical loss factor.

1 | INTRODUCTION

Eliminating or reducing wear particles determines the long-term successful functioning of artificial joints. Many methods have been used to reduce wear. One of the most effective methods is improving fluid film lubrication and thereby reducing direct asperity contact between the surfaces of artificial hip joints. Therefore, the lubrication of artificial hip joints plays a significant role in the tribological performance of hip implants.

The hip replacement works under different types of lubrication regimes, such as boundary, mixed or full-film lubrication. Various lubrication mechanisms are involved in hip replacements in daily life. Squeeze-film lubrication is an important fluid film lubrication mechanism of hip replacements, especially under heavy loads and low speeds, such as the long-time stance and the stance phase of normal daily walking cycles. Unsworth [1] pointed out that the squeeze-film lubrication action is the only fluid film lubrication mechanism which delays the direct asperity contact under conditions of start-up and stop processes. A number of theoretical studies with regard to the squeeze-film lubrication of artificial hip replacements have also been reported in the literature [2–4]. It was found that for squeeze-film lubrication problems, a lubricant pocket could be predicted, which is preferable for lubrication enhancement for the UHMWPE hip joint replacement [4]. All these studies were conducted under the assumption of elastic deformation of the UHMWPE bearing surface.

Viscoelasticity plays a significant role in both biological and engineering systems. It can be widely found in either biological systems, such as articular cartilage, or biomedical devices, such as joint replacements using UHMWPE. Significant time lags may be displayed in such soft viscoelastic materials, which may affect the tribological performance of these materials and therefore should be considered in the corresponding analyses [5]. The effects of viscoelasticity of UHMWPE on the lubrication performance of hip replacements under normal walking conditions have been investigated in a previous publication [6]. It was found that under normal walking conditions, the viscoelasticity of

UHMWPE indeed plays a significant role in the lubrication performance of soft hip implants. However, the viscoelastic effects of UHMWPE on the squeeze-film lubrication action of soft hip replacements remain unclear. Understanding the effects of the viscoelasticity of UHMWPE on the lubrication performance of hip replacements under different conditions, such as the pure squeeze condition, could provide more insights into the lubrication mechanisms in artificial hip joints using an UHMWPE liner.

Therefore, the aim herein is to investigate the effects of viscoelastic properties of a UHMWPE liner on the squeeze-film lubrication action of artificial hip replacements.

2 | MATERIALS AND METHODS

2.1 | Materials

A typical 28 mm diameter hard on soft hip replacement, consisting of a metal or ceramic head and a UHMWPE liner, was considered. The materials and geometrical properties adopted herein are listed in Table 1. The UHMWPE cup was considered for both linear elastic and viscoelastic materials for the purpose of comparison. When it was considered as a linear elastic material, its instantaneous elastic modulus was 700 MPa. For a viscoelastic material model, UHMWPE was characterised by a standard linear model. The detailed theory of the viscoelasticity of UHMWPE has been discussed in a previous study [6]. Briefly, the strain response function of the UHMWPE cup was defined as [7, 8]:

$$\varepsilon(t) = \sigma_0 J(t) \tag{1}$$

where $J(t)$ is the creep compliance function representing the time-dependent strain [$\varepsilon(t)$] under a unit constant stress (σ_o).

The creep compliance of the standard linear viscoelastic model was

$$J(t) = \frac{1}{E_2}\left[1 + \frac{E_2}{E_1}\left(1 - e^{-\frac{t}{\tau}}\right)\right] \tag{2}$$

where E_2 represents the storage modulus (instantaneous elastic modulus), E_1 the loss modulus, and τ the retardation time defined as η_u/E_1 (where η_u is the viscosity of the viscoelastic material), which can be estimated by the time required after release of stress for the strain to decrease to 1/e (0.368) of its original value [9]. Herein, to investigate the effects of relaxation time τ and mechanical loss factor E_1/E_2, a wide range of parameters (13.81–200 s for τ and 0.1–0.25 for E_1/E_2) measured in a previous experimental test [5] were adopted.

TABLE 1 Materials and geometrical parameters adopted in the numerical simulation

Femoral radius, R_H	14 mm
Radial clearance, c	40 μm
Thickness of UHMWPE liner	9.5 mm
Mechanical loss factor E_1/E_2 for the viscoelastic model	0.1–0.25
Relaxation time τ for the viscoelastic model	13.81–200 s
Instantaneous elastic modulus of UHMWPE	700 MPa
Poisson's ratio of UHMWPE	0.4

The response of a viscoelastic material to an arbitrary stress profile was obtained by decomposing the loading history into a series of small steps. The strain resulting from these small steps was superposed to obtain the final strain at time t by the Boltzmann hereditary integral [7, 8]:

$$\varepsilon(t) = \int_0^t J(t-\xi)\frac{d\sigma(\xi)}{d\xi}d\xi \tag{3}$$

2.2 | Loading and motion

Only the squeeze-film motion in the y-direction (Figure 1) was considered here. A constant load of 2000 N was applied in the same direction (w_y in Figure 1). At the beginning of the squeeze-film motion, a spherical geometrical profile with a minimum undeformed gap of 40 μm was adopted as the initial film thickness. The initial pressure distribution was assumed to be zero because no loading was applied at the beginning.

2.3 | Lubrication models

A ball-in-socket model was adopted to represent the artificial hip joint replacement (Figure 1). The lubricant was

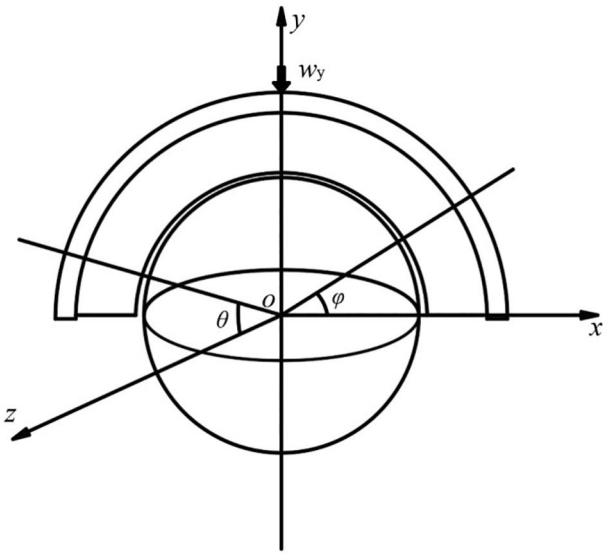

FIGURE 1 Ball-in-socket lubrication model of artificial hip joint under squeeze-film motion

periprosthetic synovial fluid and assumed to be Newtonian. A given viscosity of 0.01 Pa·s was chosen to account for the relatively small shear rate under squeeze-film motion as compared with the sliding motion [4].

As only the squeeze-film motion was considered in this study, the time-dependent Reynolds equation in the spherical coordinates was [4]:

$$\sin\theta\frac{\partial}{\partial\theta}\left(\frac{h^3}{\eta}\sin\theta\frac{\partial p}{\partial\theta}\right)+\frac{\partial}{\partial\varphi}\left(\frac{h^3}{\eta}\frac{\partial p}{\partial\varphi}\right)=12R_c^2\sin^2\theta\frac{\partial h}{\partial t} \tag{4}$$

where p is the hydrodynamic pressure; h is the lubricant film thickness; R_c is the radius of the cup; t is the time; η is the viscosity of the lubricant; and φ and θ are the spherical coordinates defined in Figure 1.

The load imposed on the acetabular cup was balanced by the integration of the hydrodynamic pressure:

$$f_x=R_c^2\int_0^{\pi}\int_0^{\pi}\rho\sin^2\theta\cos\varphi d\,\theta d\,\varphi=0 \tag{5}$$

$$f_y=R_c^2\int_0^{\pi}\int_0^{\pi}\rho\sin^2\theta\sin\varphi d\,\theta d\,\varphi=W_y(t) \tag{6}$$

The film thickness included the undeformed gap between the two bearing surfaces and the viscoelastic deformation caused by the hydrodynamic pressures:

$$h(\varphi,\theta,t)=c-e_x\sin\theta\cos\varphi-e_y\sin\theta\sin\varphi+\delta(\varphi,\theta,t) \tag{7}$$

where δ is the viscoelastic deformation of UHMWPE cup; c is the radial clearance between the cup and the head; e_x and e_y are the eccentricities of the femoral head.

2.4 | Numerical methods

The implant surfaces are typically covered by a boundary film such as a protein layer. Different mixed lubrication models were proposed to consider the direct [10] (without considering the boundary film) and indirect [11] contact (considering the boundary film) between the bearing surfaces. A boundary film thickness h_B was defined in order to consider the direct and indirect contact during the squeeze motion process [11, 12]. By assuming the boundary film thicknesses h_B as 0 and 30 nm, respectively, the effects of boundary film thickness on the numerical lubrication results were investigated. When the calculated fluid film thickness was equal to or less than the assumed film thickness h_B, it was then reset to be h_B as described in the following equation:

$$h_{i,j}=h_B\cdot\text{if}\cdot h_{i,j}<h_B \tag{8}$$

All the governing equations were non-dimensionalised in order to facilitate the numerical process and improve the convergence. It was verified that a mesh density of 240 × 240 was sufficiently accurate in previous studies [13, 14]. Therefore, a mesh density of 257 × 257 was adopted. Only one level of grid was adopted here. The finite difference method was utilised to approximate the governing equations. A point Gauss-Seidal relaxation method was used to solve the discretised Reynolds equation. The pressure convergent criterion was set as 0.0001 in order to guarantee the accuracy of numerical convergence.

In order to consider the long time stance, a relatively long time 4τ (55.24 s when the relaxation time τ was 13.81 s) was adopted for the squeeze-film lubrication analyses. The cross-sectional film thickness and pressure distributions at several time instants (t = $\tau/10$, $\tau/4$, τ, 4τ) were also output and discussed. To consider the memory effect of viscoelastic materials, the time domain (1 s) was discretised into 100 small time steps. The pressure distributions were assumed unchanged in each time step. Then the viscoelastic deformation was calculated based on the Boltzmann hereditary integral and instantaneous elastic deformation coefficients. The detailed instantaneous elastic and viscoelastic deformation calculation method was similar to that of a previous publication [6]. Briefly, the instantaneous elastic deformation coefficients of the cup surface were calculated using a finite-element method [15]. Then a unit pressure was applied on the central element of the inner surface of the cup. The displacement coefficients along the longitudinal line were used to curve fit a displacement influence function making use of the spherical distance as the independent variable. The instantaneous elastic deformation coefficients of all the nodes on the inner surface were calculated based on this function. Based on the instantaneous elastic deformation coefficients and creep compliance function, the viscoelastic deformation coefficients were obtained for each time instant over a gait cycle.

3 | RESULTS

The elastic and viscoelastic deformations calculated by the present numerical method and the finite element method (FEM) showed good consistency (Figures 2 and 3). The largest differences in the elastic and viscoelastic deformations between the numerical and FEM results were all below 0.5%.

The central film thickness and maximum pressure obtained by assuming the boundary film thickness of 30 nm showed great consistency with the predictions as 0 nm (Figure 4). When the boundary film thickness was 0 nm, the minimum film thickness decreased to 0 nm at 3.86 s. Meanwhile for the boundary film thickness of 30 nm, it was 3.59 s. Therefore, the boundary film thickness of 30 nm was adopted in order to consider the real boundary protein film [11, 16].

The minimum and central film thicknesses decreased quickly in the first few seconds, then the minimum film

thickness kept decreasing until the boundary film thickness was reached, while the central film thickness kept decreasing slowly during the entire squeeze motion process. The time required in the viscoelastic case ($\tau = 13.81$ s) to reach asperity contacts was only 15.6% of that in the elastic case (3.59 s and 23 s, respectively) (Figure 5). The central film thickness in the viscoelastic model was thicker than that of the elastic model during the entire squeeze motion process. However, the minimum film thickness in the viscoelastic model was much less than in the elastic model, which caused the asperity contact of the viscoelastic model to occur earlier than the elastic model [Figure 5(a)]. The maximum pressure of both the elastic and viscoelastic models increased quickly in the first few seconds. After the elastic model reached the maximum values (around 7.7 MPa), it did not change with time any further. In contrast, the maximum pressure of the viscoelastic model reached a peak value of 7.4 MPa in less than 1 s, then kept decreasing until reaching a steady value of around 5.3 MPa [Figure 5(b)].

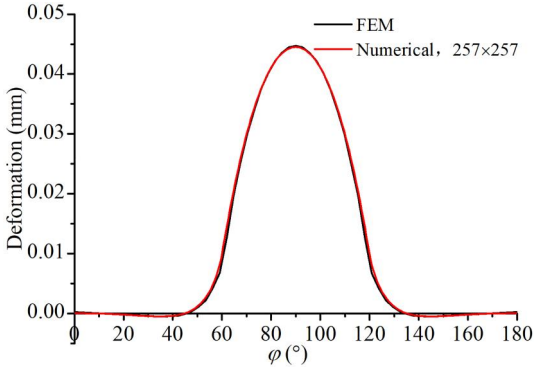

FIGURE 2 The cross-sectional instantaneous elastic deformation of the UHMWPE cup under a parabolic pressure distribution with the maximum pressure of 10 MPa and a half contact angle of 30°

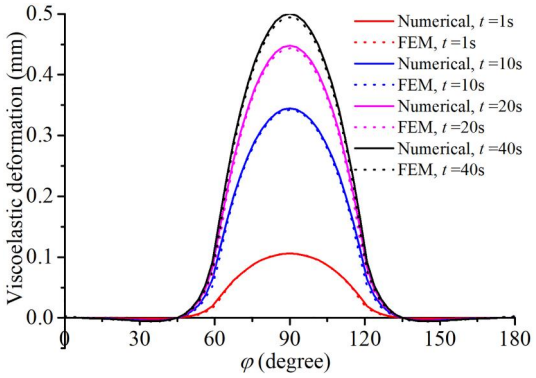

FIGURE 3 The cross-sectional viscoelastic deformation of the UHMWPE cup under a parabolic pressure distribution with the maximum pressure of 10 MPa and a half contact angle of 30°

From the cross-sectional film thickness and pressure distributions at several time instants (1.38 s, 3.45 s, 13.81 s, 55.24 s), it was further confirmed that the film thicknesses of the viscoelastic model were generally larger than those of the elastic model, however the minimum film thickness of the viscoelastic model was smaller than the elastic model [Figure 6(a)]. A film constriction area formed near the outlet of the contact area is shown in Figure 6(a) (the red rectangle area). A relatively large change in the pressure was obvious at the constriction area at the instant of 13.81 s (Figure 6(b)). The position of the minimum film thickness of both models appeared inside the film constriction area. The contact area of the elastic model was nearly constant during the squeeze-film motion process. However, the contact area of the viscoelastic model gradually increased as time increased (Figure 6). From the comparisons of the cross-sectional film thickness and pressure distributions of the viscoelastic model between 13.81 s and 55.24 s, the changes in the film thickness and pressure distributions were negligible. However, the lubricant pole at the edge of the contact area became much flatter at 55.24 s compared with 13.81 s.

With the increase in relaxation time, the time-dependent minimum and central film thicknesses of the viscoelastic model became closer to those of the elastic model. For a smaller relaxation time, it took a shorter time for the minimum

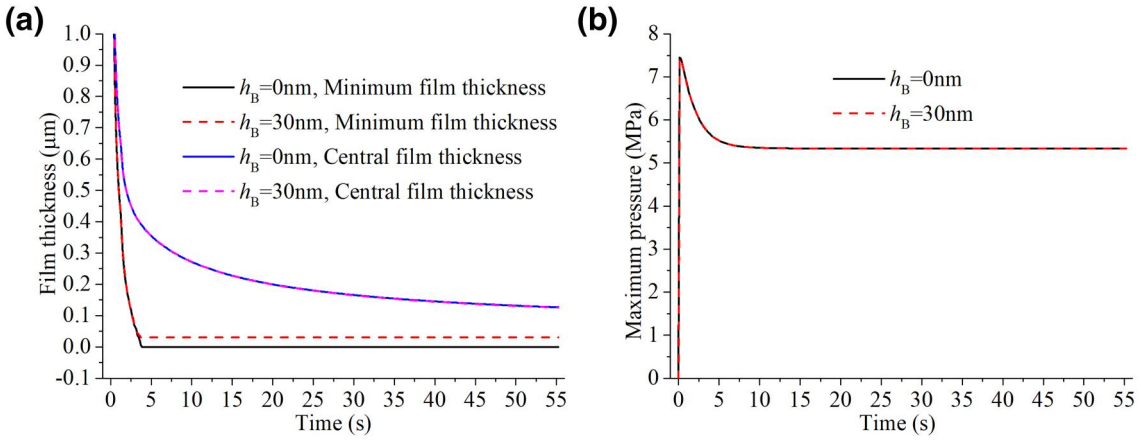

FIGURE 4 (a) Minimum and central film thicknesses and (b) maximum pressures under different boundary film thickness

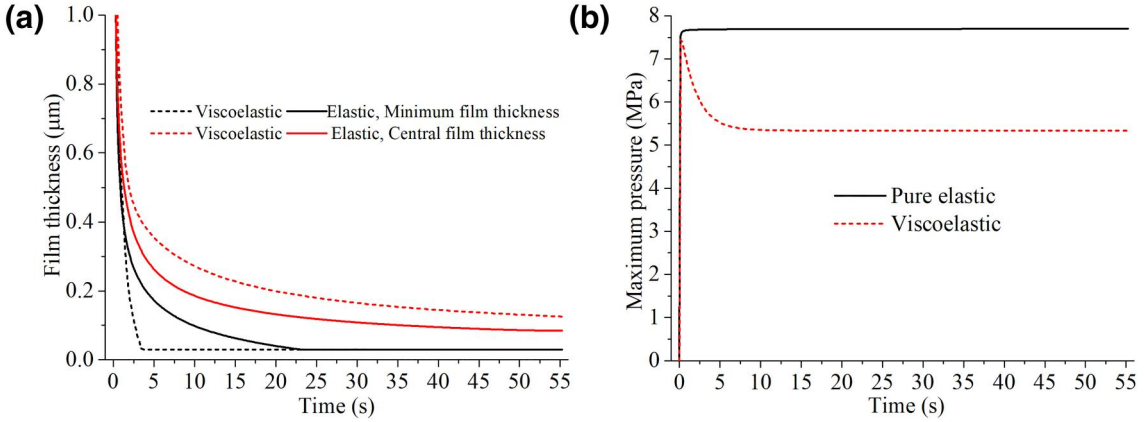

FIGURE 5 (a) Minimum and central film thicknesses and (b) maximum pressures when the UHMWPE cup was assumed as pure elastic and viscoelastic materials

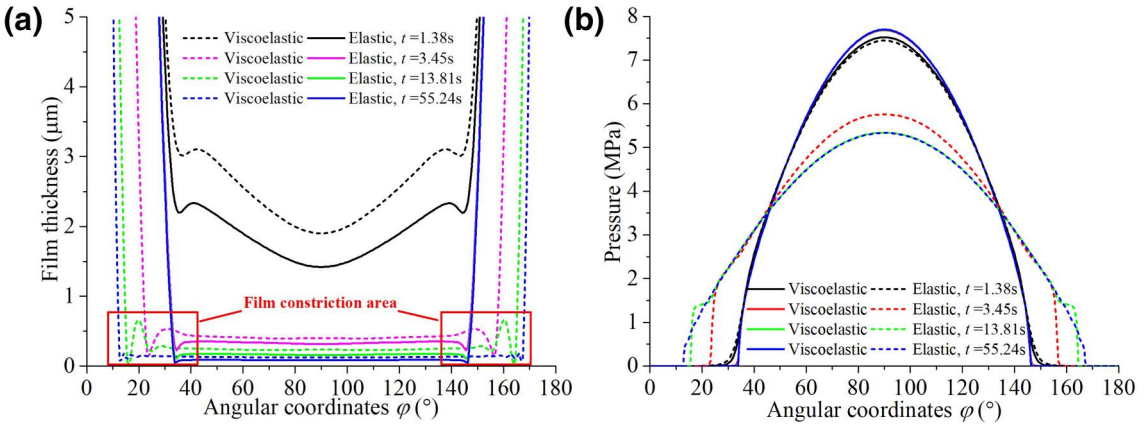

FIGURE 6 (a) The cross-sectional film thicknesses and (b) pressures at four time instants (t =1.38, 3.45, 13.81, 55.24 s, relaxation time τ =13.81 s)

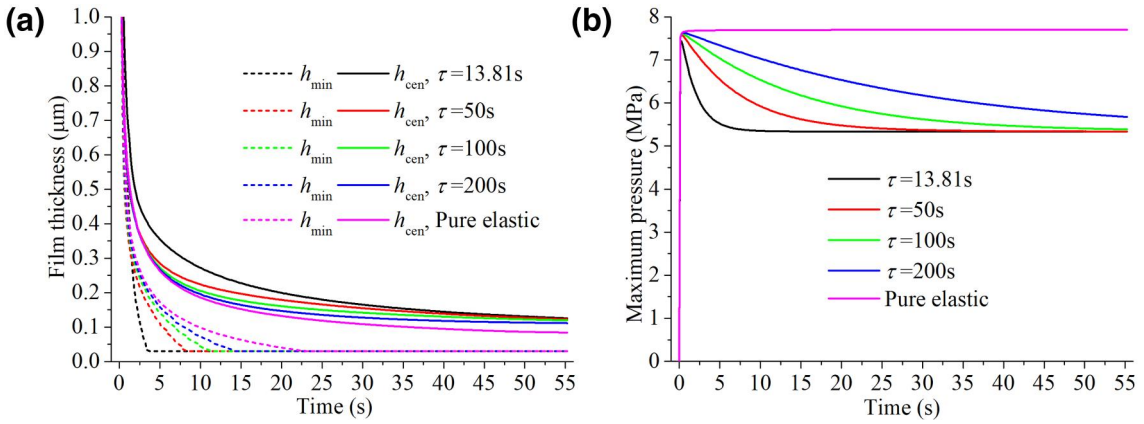

FIGURE 7 (a) The minimum and central film thicknesses and (b) maximum pressures of the elastic and viscoelastic models for different relaxation times under squeeze-film motion

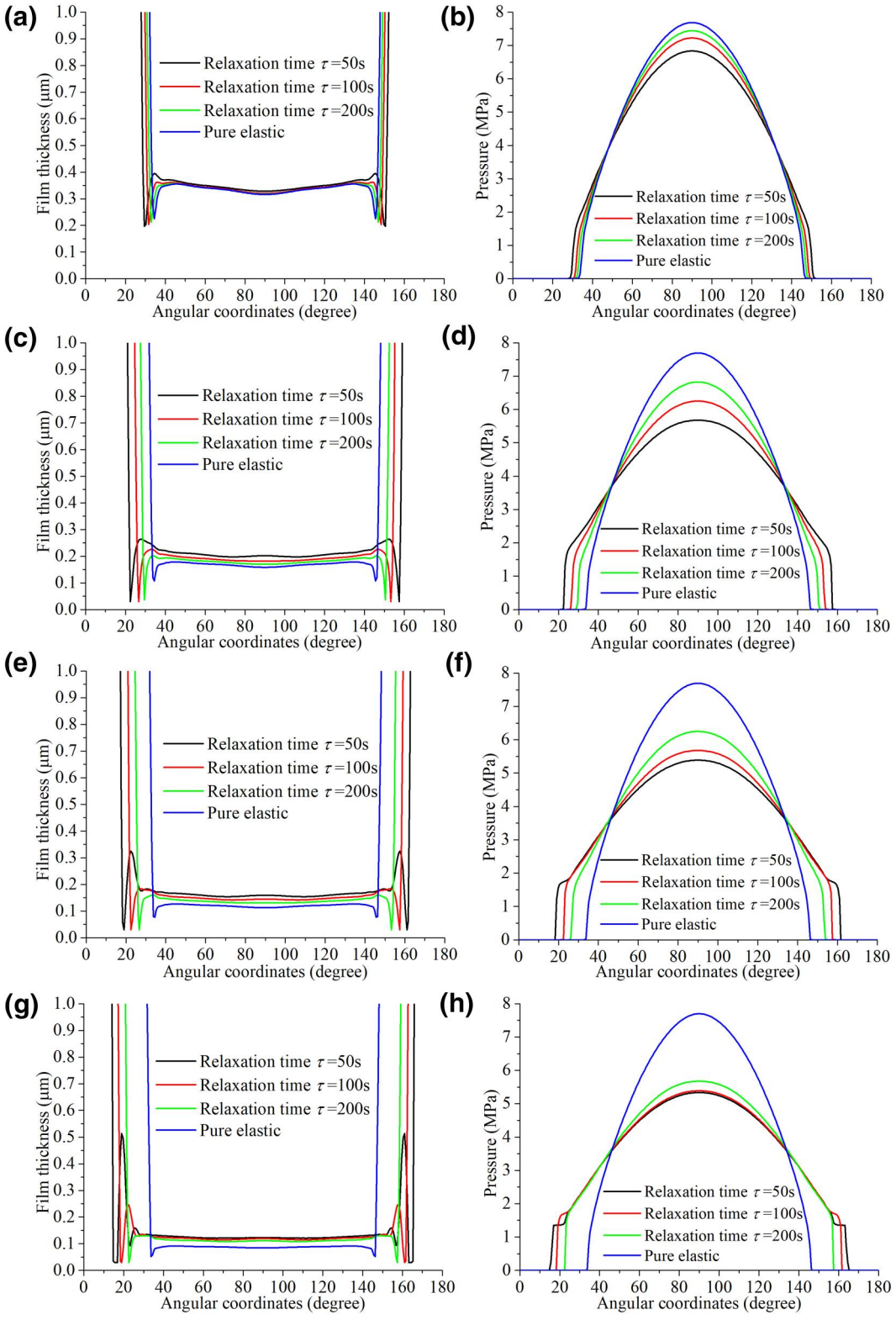

FIGURE 8 The comparison of the cross-sectional film thicknesses (a) 3.45 s, (c) 13.81 s, (e) 27.62 s, (g) 55.24 s and cross-sectional pressures (b) 3.45 s, (d) 13.81 s, (f) 27.62 s, (h) 55.24 s between the viscoelastic model and the elastic model

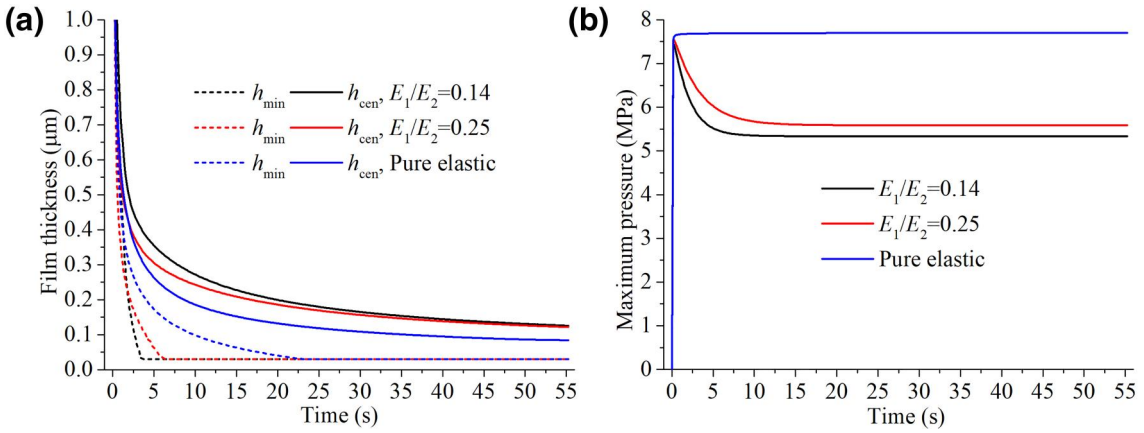

FIGURE 9 (a) The comparison of minimum and central film thicknesses and (b) maximum pressures under squeeze-film motion between different mechanical loss factors (E1/E2)

film thickness to reach the assumed boundary film thickness h_B (Figure 7(a)). Correspondingly, the maximum pressure of the model with smaller relaxation times took less time to reach the equilibrium value (around 5.3 MPa). It took 3.59 s for the minimum film thickness to reach the boundary film thickness h_B when the relaxation time was 13.81 s. Meanwhile, for the relaxation time of 50 s, 100 s, and 200 s, the time taken was 8.42 s, 11.46 s, and 14.08 s, respectively (Figure 7).

Furthermore, the contact area became larger with the decrease in relaxation time. In addition, the lubricant pocket at the edge of the contact area became more obvious (Figure 8). For all the instants investigated, the maximum pressure decreased as the relaxation time reduced (Figure 8). The differences in the maximum pressure between the cases with the relaxation times of 50 s, 100 s, and 200 s became smaller as time increases (Figure 8).

The minimum film thickness decreased to the boundary film thickness at 3.59 s and 6.21 s when the mechanical loss factor was 0.14 and 0.25, respectively. The maximum pressures of almost all the models increased to the peak value of around 7.5 MPa instantaneously. Then the maximum pressure of the elastic model kept constant, while those of the viscoelastic models with mechanical loss modulus of 0.14 and 0.25 decreased gradually and reached the finalequilibrium values of 5.33 and 5.58 MPa, respectively (Figure 9).

The contact area became larger with a decrease in the mechanical loss factor (Figure 10). After the maximum pressure reached the equilibrium value, the difference between the selected two viscoelastic models was around 0.25 MPa and kept nearly constant (Figure 9). This difference can also be seen from the cross-sectional pressure distribution. Although the pressure profiles have differences, the maximum pressure differences were all around 0.25 MPa (Figure 10).

4 | DISCUSSION

n a previous study [6], the transient lubrication simulation under normal walking conditions was investigated. However, the pure squeeze-film motion is another important scenario, which exists in the long-time standing period and the stance phase of the normal daily walking cycles. Understanding the effects of the viscoelasticity of UHMWPE on the lubrication performance of hip replacements under the pure squeeze condition could provide more insights into the lubrication mechanisms of artificial hip joints using a UHMWPE liner. Therefore, a viscoelastic squeeze-film lubrication model of UHMWPE artificial hip replacements was developed here, and the effects of viscoelastic parameters on the squeeze-film lubrication performance were also discussed.

As the squeeze motion proceeded, the lubricants flowed out from the contact area and formed a film constriction near the outlet. As a result, the minimum film thickness appeared at the position of constriction. The constriction area was very small and, therefore, the adopted boundary film thickness (0 and 30 nm) had little effect on the central film thickness and maximum pressure.

The viscoelastic property of the UHMWPE liner had considerable effects on the squeeze-film lubrication of artificial hip replacements. The deformation at the present instant was based on the deformed surfaces caused by the loading of the previous instants. Therefore, the deformation at the present instant was determined by the present loading and previous loadings. Due to the synergistic effects of residual deformations at previous time instants and constant loading, a smaller minimum film thickness appeared in the viscoelastic model. Therefore, the direct contact of the bearing surfaces of the viscoelastic model occurred earlier than the elastic model during the squeeze motion process. As the lubricants flowed out from the contact area, the lubricant pocket was enhanced

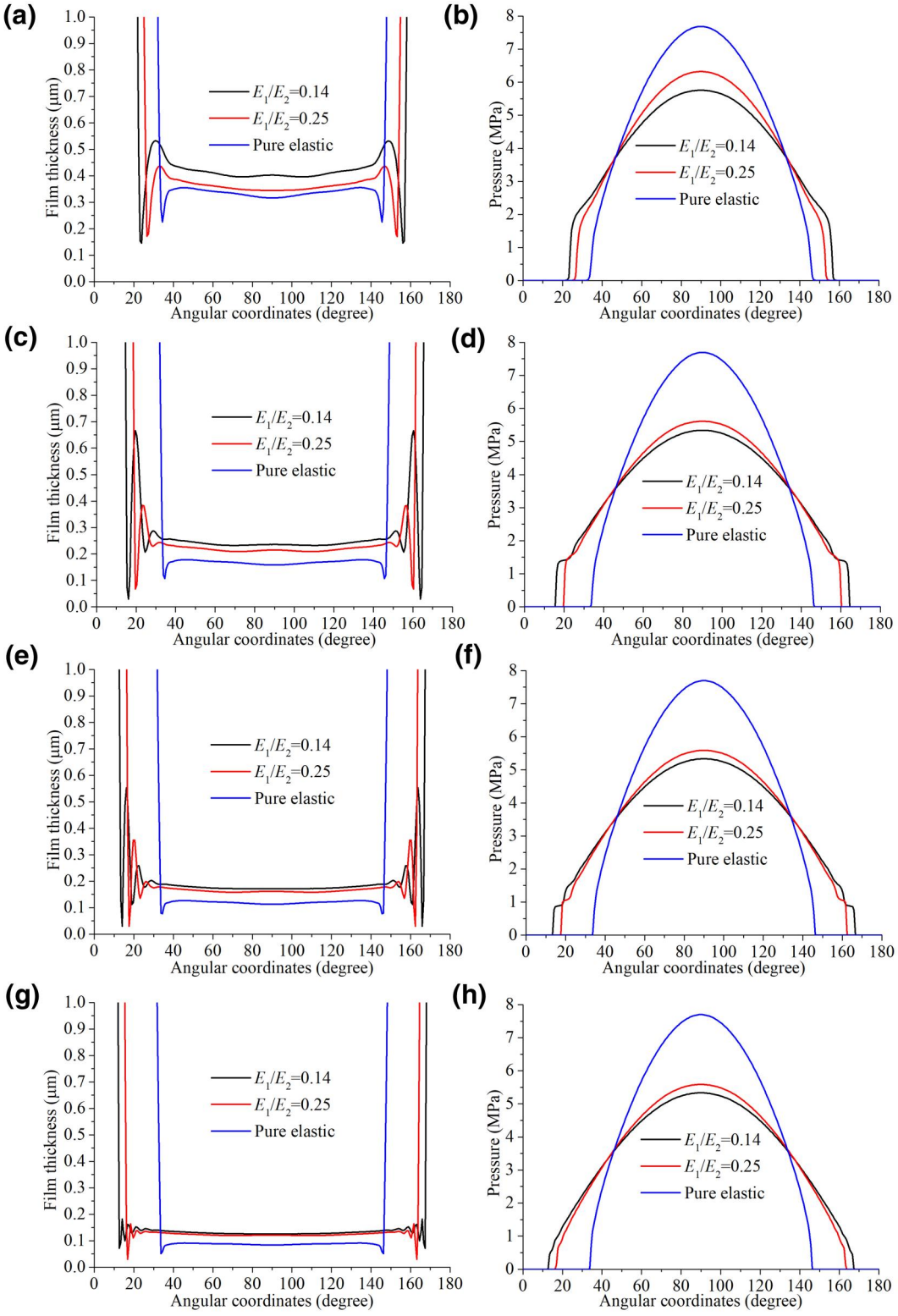

FIGURE 10 The cross-sectional film thicknesses (a) 3.45 s, (c) 13.81 s, (e) 27.62 s, (g) 55.24 s and pressures (b) 3.45 s, (d) 13.81 s, (f) 27.62 s, (h) 55.24 s at several instants for different mechanical loss factors

at the position close to the constriction area. Due to the restriction of the constriction area at the outlet, the lubricant of the viscoelastic model was more difficult to flow out from the contact area. As a result, the central film thickness of the viscoelastic model was thicker than the elastic model.

For both the elastic and standard linear model, an instantaneous elastic deformation occurred as the load applied. Therefore, for both models, the maximum pressures increased to the peak value in a short time period. Furthermore, the film thickness and pressure distributions of the viscoelastic model were similar to those of the elastic model at the beginning of squeeze-film motion. Due to the restriction of the constriction area at the outlet to the fluid flow, a steep pressure gradient had to be formed at the constriction area to satisfy the continuity of the fluid. Therefore, relatively large pressure changes appeared at the constriction area of both the elastic and viscoelastic models. However, as the squeeze-film motion proceeded, these squeeze-film phenomena (i.e., the relatively large changes in the pressure and lubricant pocket towards the edge of the contact) became more obvious in the viscoelastic model due to accumulation of the viscoelastic deformation. Moreover, such a change in pressure with time seemed to be consistent with previous contact mechanics analysis [7].

As the elastic deformation reached the maximum value and kept constant, the maximum pressure of the elastic model was also a constant. However, the contact area of the viscoelastic model kept increasing with the increase in viscoelastic deformation. As a result, the maximum pressure of the viscoelastic model kept decreasing with the increase in the contact area until the complete release of the viscoelastic deformation.

Assuming a fixed mechanical loss factor, it took a shorter time for the viscoelastic model to reach the same maximum deformation for a smaller relaxation time. As a result, the direct contact occurred earlier as the relaxation time decreased. Likewise, the maximum pressure took less time to reach the equilibrium status. At the same time instant, the viscoelastic deformation became larger as the relaxation time decreased, causing an increase in the contact area and a decrease in the maximum pressure.

The mechanical loss factor also had obvious effects on the squeeze-film lubrication action of artificial hip joints. Under the assumption of fixed relaxation time, the equilibrium value of maximum pressure was mainly determined by the loss modulus. With an increase of loss modulus, the final equivalent elastic modulus became larger, which caused an increase in the final maximum pressure. The viscoelastic model took a longer time to reach the maximum deformation for a large mechanical loss factor. Therefore, a direct contact occurred later with an increase in the mechanical loss factor.

There are a few limitations in the present study. Firstly, the bearing surfaces were assumed as smooth in the numerical analyses. Secondly, a Newtonian lubricant model was assumed, while the rheology property of synovial fluid was much more complex. In addition, a constant loading was adopted in the squeeze-film lubrication analyses. Despite these limitations, it was clear that the viscoelasticity of the UHMWPE liner has important effects on the squeeze-film lubrication action of hip replacements.

5 | CONCLUSIONS

A viscoelastic squeeze-film lubrication model has been developed and solved in order to investigate the influence of viscoelasticity of a UHMWPE liner on the squeeze-film lubrication performance of soft artificial hip replacements. The main findings include:

The viscoelasticity had negative effects on the minimum film thickness and caused the direct contact earlier, while it was beneficial for enhancement of the central film thickness.

Different from the elastic model, the maximum pressure of the viscoelastic model increased to the maximum value and decreased to the second equilibrium status, which was determined by the time-dependent viscoelastic deformation behaviour of UHMWPE.

The decrease in the relaxation time and mechanical loss factor resulted in the enhanced effect of the viscoelastic lubricating performance.

ACKNOWLEDGEMENTS

The work was supported by National Science Foundation of China [grant number 51323007], and National Science and Technology Supporting Programme [grant number 2012BAI18B00].

ORCID

Xianjiu Lu https://orcid.org/0000-0003-3326-6035

REFERENCES

1. Unsworth, A.: Tribology of human and artificial joints. J. Eng. Med. (1991)
2. Mabuchi, K., Sasada, T.: Numerical analysis of elastohydrodynamic squeeze film lubrication of total hip prostheses. Wear. 140, 1–16 (1990)
3. Wang, C.-T., et al.: Calculation of elastohydrodynamic lubrication film thickness for hip prostheses during normal walking. Tribol. Trans. 33, 239–245 (1990)
4. Jagatia, M., Jalali-Vahid, D., Jin, Z.M.: Elastohydrodynamic lubrication analysis of ultra-high molecular weight polyethylene hip joint replacements under squeeze-film motion. Proc. Inst. Mech. Eng. H. 215, 141–151 (2001)
5. Deng, M., Uhrich, K.E.: Viscoelastic behaviours of ultrahigh molecular weight polyethylene under three-point bending and indentation loading. J. Biomater. Appl. 24, 713–732 (2010)
6. Lu, X., et al.: Transient viscoelastic lubrication analyses of UHMWPE hip replacements. Tribol. Int. 128, 271–278 (2018)
7. Chen, W.W., et al.: Semi-analytical viscoelastic contact modelling of polymer-based materials. J. Tribol. 133 041404 (2011)
8. Brinson, H., Brinson, L.: Polymer Engineering Science and Viscoelasticity: an Introduction. Springer (2008)
9. Gooch, J.W.: Retardation time. In: Gooch, J.W., (ed.) Encyclopedic Dictionary of Polymers, pp. 627–627. Springer New York, New York (2011)

10. Wang, F.C., Jin, Z.M.: Lubrication modelling of artificial hip joints. IUTAM Symposium on Elastohydrodynamics and Micro-elastohydrodynamics, 385–96 (2006)
11. Wang, F.C., et al.: Lubrication and friction prediction in metal-on-metal hip implants. Phys. Med. Biol. 53, 1277–1293 (2008)
12. Gao, L., et al.: Effect of surface texturing on the elastohydrodynamic lubrication analysis of metal-on-metal hip implants. Tribol. Int. 43, 1851–1860 (2010)
13. Liu, F., et al.: Transient elastohydrodynamic lubrication analysis of metal-on-metal hip implant under simulated walking conditions. J. Biomech. 39, 905–914 (2006)
14. Liu, F., et al.: Transient elastohydrodynamic lubrication analysis of a metal-on-metal hip implant under simulator-tested conditions. In: Proceedings CDROM of the Sixth World Congress on Computational Mechanics in Conjunction with the Second Asian-Pacific Congress on Computational Mechanics, Beijing (2004)
15. Wang, F.C., Jin, Z.M.: Prediction of elastic deformation of acetabular cups and femoral heads for lubrication analysis of artificial hip joints. Proc. IME. JJ. Eng. Tribol. 218, 201–209 (2004)
16. Mattei, L., et al.: Lubrication and wear modelling of artificial hip joints: a review. Tribol. Int. 44, 532–549 (2011)

How to cite this article: Lu, X., Meng, Q., Jin, Z.: Effects of UHMWPE viscoelasticity on the squeeze-film lubrication of hip replacements. Biosurface and Biotribology. 7, 60–69 (2021). https://doi.org/10.1049/bsb2.12006